ENERGY EVALUATION OF SHOCK WAVE EMISSION AND BUBBLE GENERATION BY LASER FOCUSING IN LIQUID NITROGEN

Y. Tomita[*], M. Tsubota[**] and N. An-naka[***]
[*] Hokkaido University of Education, Hakodate 040-8567, Japan
[**] Osaka City University, Osaka 558-8585, Japan
[***] JGC Corporation, Yokohama 220-6001, Japan

Abstract

When the energy level of a laser beam at the focus exceeds an irradiance threshold the optical breakdown occurs, followed by a series of high-speed phenomena such as plasma formation, shock wave emission and vapor bubble generation. In this paper the energy evaluation associated with these phenomena has been made for laser focusing in liquid nitrogen. It is found that the threshold laser energy capable of bubble formation has an extent with some probability, tending to decrease with increasing the applied pressure. The mechanical energies of shock wave emission and bubble generation have been investigated.

1 Introduction

Recently the study of cavitation in cryogenic fluids has been widely noticed by many researchers in the field of space engineering where the cryogenic fluids frequently flow with high-speed in a pipe, resulting in gas-liquid two phase flow. This requires a better knowledge of the bubble dynamics in cryogenic fluids. As is generally known lasers have a merit of producing a highly spherical bubble (Lauterborn 1974; Vogel, Lauterborn & Timm 1989, Tomita & Shima 1990; Philipp & Lauterborn 1998; Isselin,Alloncle & Autric 1998), then several attempts have been performed on the bubble dynamics in liquid nitrogen, which is one of the most common cryogenic fluids (Golubnitchii et al.1979; Maeno, Yokoyama & Hanaoka 1990; Tomita et al. 1994; Sato et al.1996). Tomita and his co-workers investigated the behavior of laser-induced cavitation bubbles together with the high-speed fluid phenomena induced in liquid nitrogen (Tsubota et al. 1996; Tsubota, An-naka & Tomita1996; Tomita et al. 2000). Although the majority of sophisticated investigations has been carried out for water by Vogel and his coauthors (Vogel, Busch & Parlitz 1996; Vogel et al. 1999), there are no reports on the energy consideration for cryogenic fluids. In this paper we address the energy consideration of the laser-induced fluid phenomena in liquid nitrogen, especially regarding the threshold energy for bubble generation and the evaluation of mechanical energies of shock wave emission and bubble generation.

2 Experimental Facilities and Method

Figure 1 shows a schematic view of the experimental apparatus. Liquid nitrogen was filled in an aluminum test chamber with the inner dimension of 105mm x 105mm x 110mm, which was equipped at the lower part of a cryostat made of stainless steel, having 794mm in total length and 460mm in outer diameter. The chamber was designed for enduring the external pressure up to 304kPa and for preserving the space between the test chamber and the outside walls of the cryostat being at high vacuum, 6.7×10^{-4}Pa, to insulate heat from the surroundings. The temperature of the bulk liquid nitrogen was monitored by employing a Pt resistance thermometer (Lake Shore, PT102-14D) and

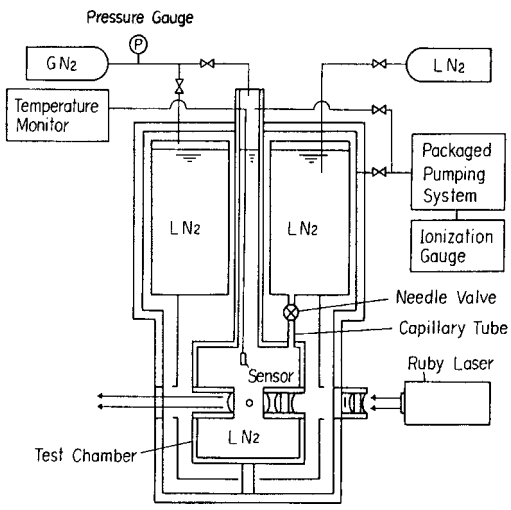

Figure 1. Schematic view of the experimental apparatus.

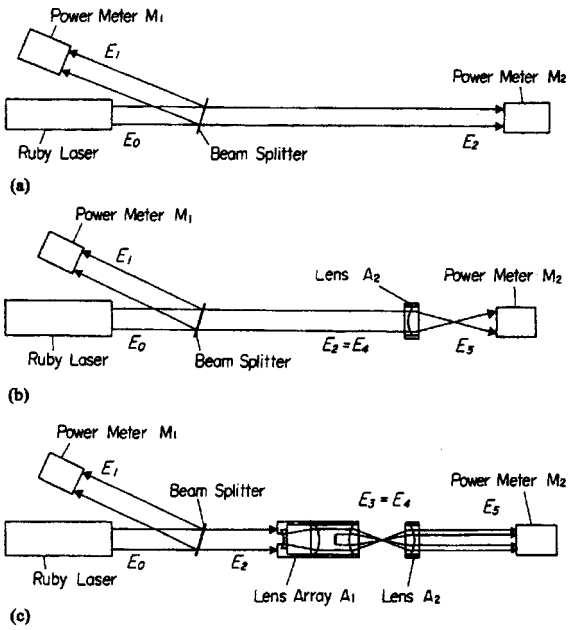

Figure 2. Method of optical energy measurement.

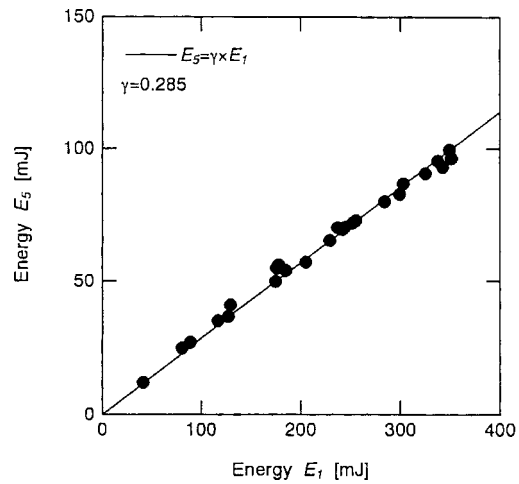

Figure 3. Correlation between the energies E_1 and E_5.

the boiling temperature of the liquid nitrogen was measured at 78.0K. In the present experiment, a Q-switched ruby laser (Japan Science Engineering Co. Ltd., NAL-707TS1, wavelength 694nm) with 30ns full width at half maximum pulse duration in single - mode TEM_{00} operation was used for generating a bubble in liquid nitrogen. In order to produce a highly spherical bubble, a double stage of lens system was inserted along the axis of the laser beam (Tomita et al. 1994; Tsubota et al.1996). The laser beam was finally focused with a larger convergent angle of 38.3degrees. The spot diameter of the laser beam at the focus was about 20micron (Tomita et al. 2000) measured by using knife-edge technique (Siegman, Sasnett & Johnston Jr. 1991).

Figure 2 shows three setups of optical alignment for laser energy measurement. The laser energies were basically detected with two sets of power meters (Japan Science Engineering Co.Ltd., PM-322, accuracy 0.1mJ). Figure 3 shows the correlation between the energies E_1 ($=E_{ref}$) and E_5 ($=E_{col}$) obtained from the whole system indicated in Figure 2(c). The laser energy, E_c, was consumed at the focus due to the interaction between the laser beam and the molecules of liquid nitrogen, which is equivalent to the energy difference, $E_{in}-E_{out}$, with E_{in} being the input laser energy, that is the energy of the laser beam just entering the liquid nitrogen, and E_{out} the transmitted laser energy. Consequently, the consumed laser energy E_c can be written in terms of E_{ref} and E_{col} as follows:

$$E_c = E_{in} - E_{out} = 0.307E_{ref} - 1.636\,E_{col} \tag{1}$$

The energies of E_{ref} and E_{col} were measured with two power meters, M1 and M2. It is reasonably considered that the energy E_c can be divided into the following individual energies: (1) the work done by the liquid displaced during the bubble expansion, which is called the bubble energy E_B, (2) the shock wave energy E_S, (3) the surface energy, (4) the light energies associated with stimulated Brillouin scattering, plasma radiation and thermal radiation from the mixed gas with high temperature, (5) the evaporation energy and heat conduction energy, (6) the energy absorption in the liquid except near the focus, and so on. It is found that when a cavitation bubble was created, about 80% of the input laser energy, E_{in}, was consumed at the focus and even in the case where no bubble generation was achieved, about 25% of the input laser energy was dissipated owing to the laser beam-nitrogen molecules interaction. The irradiance density defined by taking the input laser energy E_{in} as a threshold energy is given as

$$I = \frac{E_{in}}{\pi w_0^{\,2} t_p} \tag{2}$$

where w_0 is the spot radius of the laser beam and t_p (=30ns) the full width at half maximum pulse duration. Figure 4 shows a block diagram of the optical system for taking photographs. A shadowgraph technique was utilized for visualizing the phenomena taken by an image converter high-speed camera (John Hadland, Imacon 790) with the framing rate of 5,000,000 frames/s and with the streaking rate of 10x 10^{-6}sec/cm. A mechanical shutter positioned between an argon-ion laser and the cryostat produced a signal when it opened for triggering the events. The signal was branched into two, each delivering to the camera and to the ruby laser. Synchronization with the phenomena was adjusted with a delay circuit because the laser has a characteristic time delay of about 850 x 10^{-6}sec from receiving the signal. Since it is well known that the time interval between the first two peaks of a pressure-time history caused by the bubble motion is accurately corresponding to the first period of the bubble oscillation (Vogel, Lauterborn & Timm 1989; Tomita & Shima 1990; Tomita et al. 1994), which is proportional to the maximum bubble radius, the pressure measurement was conducted by employing a pressure transducer (PCB, 113M186) positioned at 10mm from the bubble generation.

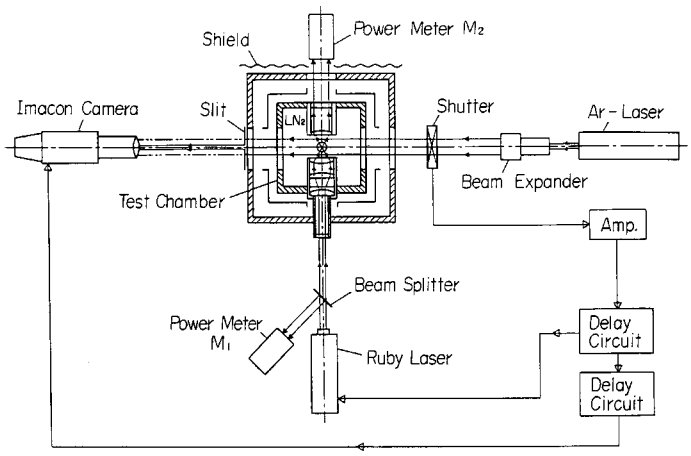

Figure 4. Optical system for observation.

3 Evaluation of Bubble Energy and Shock Wave Energy

3.1 Cavitation bubble energy

The work done by the displaced liquid nitrogen during the expansion of a bubble from the initial radius R_0 to the maximum radius R_{max} against ambient pressure p_∞, which is termed as the bubble energy E_B, can be expressed by

$$E_B = \int_{R_0}^{R_{max}} 4\pi R^2 p_\infty dR = \frac{4\pi p_\infty}{3}\left(R_{max}^3 - R_0^3\right) \cong \frac{4\pi}{3} R_{max}^3 p_\infty \qquad (3)$$

because the initial bubble radius R_0 was supposed to be equaled the radius of a plasma with 10^{-5}m, which is negligibly small in comparison with R_{max}. Furthermore when a bubble is subject to an inertially dominated motion of the liquid, R_{max} is known to be linearly proportional to the period of the bubble motion, T_B, as follows (Rayleigh 1917):

$$R_{max} = \frac{T_B}{1.83}\sqrt{\frac{p_\infty - p_v}{\rho_\infty}} \qquad (4)$$

where ρ_∞ is the liquid density and p_v the vapor pressure of the liquid. For liquid nitrogen the validity of Eq. (4) was confirmed by the authors (Tomita et al. 1994).

3.1 Shock wave energy

After a plasma is formed, it rapidly expands during the laser pulse. A vapor bubble is subsequently generated as a result of the relaxation of the plasma. Since this process accelerates the liquid surrounding the bubble, a shock wave is formed, propagating outwards into the liquid nitrogen. During the very early stage of the bubble growth, a highly enthalpy flow may be produced in the liquid behind the shock wave.

The shock wave energy is defined as the energy flux across area where a shock wave front arrives at and it is expressed in the following form by applying the Rankine-Hugoniot conditions at the shock front (Cole1948),

$$E_S = \frac{4\pi r_S^{\,2}}{\rho_\infty}\int_0^{t'} \frac{(p-p_\infty)^2}{U_S - \left(\dfrac{p-p_\infty}{\rho_\infty U_S}\right)}dt \tag{5}$$

where U_s is the shock wave velocity, r_S the radial distance of the shock front from the origin and time t is taken as zero at the shock front. The equation of state for liquid nitrogen can be expressed in the form of a Tait equation given by

$$\frac{p+B}{p_\infty + B} = \left(\frac{\rho}{\rho_\infty}\right)^n \tag{6}$$

with the constants of n =18.9 and B = 37MPa which were determined by using the isothermal data on pressure-density relationship (Angus et al. 1977), since the constant n is related to the isothermal constant n_T multiplied by the ratio of specific heats, κ, leading to $n=\kappa\, n_T$. Using the conservation equations of mass and momentum, the pressure behind the shock front, p_s, can be connected with the shock wave velocity, U_s, as follows:

$$p_S - p_\infty = \left(\frac{\rho_\infty}{\rho}\right)(\rho - \rho_\infty)\cdot U_S^{\,2} \tag{7}$$

Applying the Rankine-Hugoniot's relation to Eq.(7) with the help of the Tait equation, Eq.(6) , we finally obtain

$$p_S = (p_\infty + B)\left\{\frac{2nU_S^{\,2}}{(n+1)c_\infty^{\,2}} - \left(\frac{n-1}{n+1}\right)\right\} - B \tag{8}$$

where c_∞ is the sound velocity of the undisturbed liquid nitrogen. This equation is very useful when the pressure behind the shock front is unknown, but the shock wave velocity is known. The shock wave energy E_s will be calculated by integrating Eq. (5) on the assumption that the shock wave pressure $p(t)$ varies in the form of exponential decay with respect to time t given as

$$p(t) - p_\infty = (p_S - p_\infty)\exp\left[\frac{-t\cdot\ln 2}{t_s}\right] \tag{9}$$

where t_s is the full width at half maximum pulse duration of a shock wave (i.e. the time satisfying the condition p =(p_s+ p_∞)/2). Although it may be true that the rapid expansion of a plasma could send a shock wave into the liquid layer, but in this paper we only refer to the shock wave emission due to the adiabatic expansion of a vapor bubble with no account of phase change at the bubble surface as well as without consideration of heat and mass transfer across the bubble surface. The width t_s can be approximately evaluated by solving the bubble growth in a compressible liquid nitrogen whose motion is governed by a non-linear wave equation with respect to the velocity potential ϕ given by

$$\frac{\partial^2\phi}{\partial r^2} + \frac{2}{r}\cdot\frac{\partial\phi}{\partial r} = \frac{1}{c^2}\left[\frac{\partial^2\phi}{\partial t^2} + 2\left(\frac{\partial\phi}{\partial r}\right)\cdot\left(\frac{\partial^2\phi}{\partial r\partial t}\right) + \left(\frac{\partial\phi}{\partial r}\right)^2\frac{\partial^2\phi}{\partial r^2}\right] \tag{10}$$

where r is the radial distance and c the local sound velocity. As carried out by Tomita & Shima (1977) and Fujikawa & Akamatsu (1980), the PLK method (Tsien 1956) was applied to obtain an approximate solution of the non-linear wave equation with the second-order correction of liquid compressibility.

At the location sufficiently far from the laser focusing, we are allowed to use the following expression written by the acoustic approximation for evaluating the shock wave energy instead of Eq.(5):

$$E_S = \frac{4\pi r_S^{\,2}}{\rho_\infty c_\infty}\int_0^{t'}\left(p - p_\infty\right)^2 dt + \frac{4\pi r_S^{\,2}}{\rho_\infty r_S}\int_0^{t}\left(p - p_\infty\right)\left[\int_0^{t'}\left(p - p_\infty\right)dt\right]dt' \tag{11}$$

In the above the second term on the right hand side corresponds to the afterflow effect induced by the outward spherical wave. In the field of underwater explosion it is well known that the afterflow effect is negligibly small in the region beyond the 10-20 times charge radius (Cole 1948).

4 Results and Discussion

Figure 5 shows two typical examples of shadowgraphs taken with the framing rate of 5,000,000 frames/s with the interframe time 200ns and exposure 40ns, indicating the vapor bubble formation immediately after the optical breakdown for the overpressure of Δp=4.9kPa. A laser beam was coming from the right. When the energy level of the laser beam at the focus exceeds an irradiance threshold, the optical breakdown occurs in the liquid nitrogen, followed by plasma formation. On the second frame of Figure5(a), an intense flash occurs. As clearly seen, Figure 5(a) corresponds to the case where a relatively weak interaction occurred between the laser beam and the nitrogen molecules, creating a slender cavity along the axis of the laser beam. On the other hand, several small flashes can be seen on the second frame of Figure 5(b). These flashes are probably sonoluminescence resulting from stimulated Brillouin scattering (Mainster et al. 1983; Barber & Putterman 1991; Gaitan et al. 1992). It is generally recognized that the shape of a plasma is apt to be ellipsoidal reflecting the time dependency of the intensity of the laser beam at the focus. Subsequently, a strong shock wave, whose velocity during the early period of 200-400ns was measured as 1675m/s at r_s=0.53mm which corresponded to the Mach number of 1.80 since the sound velocity of liquid nitrogen was 928m/s at T_∞=78K , is emitted. The pressure behind the shock front was calculated to be 158MPa. Figure 6 shows the shock wave pressure calculated for Figure 5(b). The relationship between the input laser energy E_{in} and the consumed energy at the focus E_c is shown in Figure 7 for Δp=4.9kPa and in Figure 8 for Δp=58.8kPa. In both cases where no bubbles were generated the energy dissipated through the liquid nitrogen was treated as the consumed energy E_c. In these figures a solid circle means the case for bubble generation, an open triangle corresponds to the case for small cavity formation (see Figure 5(a)) and a cross implies the case of no bubble generation. Furthermore E_{t1} and E_{t2}

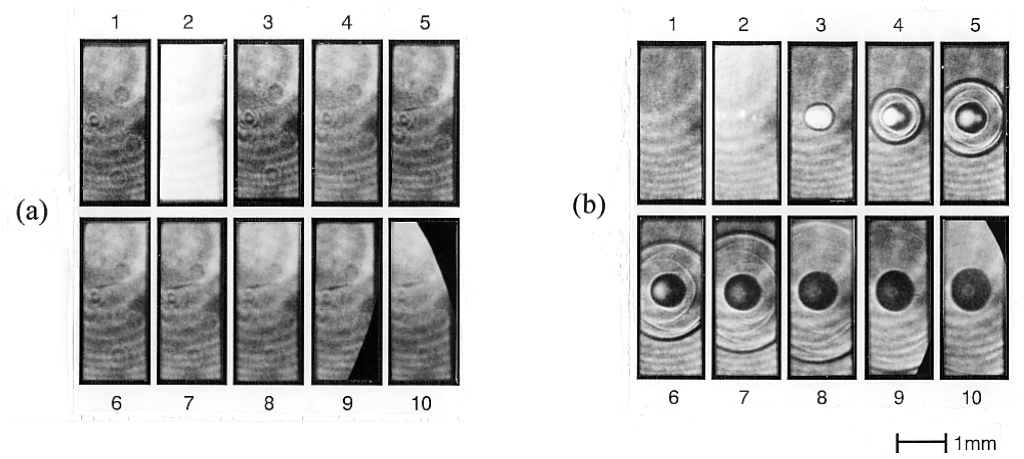

Figure 5. Bubble generation by laser focusing into liquid nitrogen :
(a) Δp=4.9kPa; (b) Δp=4.9kPa and R_{max}=2.08mm.

denote the threshold energies responsible for the situation where if the input laser energy E_{in} satisfies the condition of $E_{in} \leq E_{t1}$ no bubbles were formed. On the other hand, when the input laser energy E_{in} is given in the range of $E_{t2} \leq E_{in}$ bubbles were always generated. In the case of the middle energy condition such as $E_{t1} \leq E_{in} \leq E_{t2}$, bubbles were generated with some probability. A significant difference is found in the threshold energies in Figures 7 and 8, indicating that as increasing the overpressure Δp, an obvious increase in E_{t1} can be seen whereas a definite decrease in E_{t2} is observed. Eventually the energy difference, E_{t2}-E_{t1}, decreases as increasing Δp. Generally, it is recognized that the irradiance threshold is influenced by the inhomogeneity of liquid medium and it must be connected with the ionization energy of molecules. In particular the pressurized liquid nitrogen tends to be stabilized due to the decrease in density fluctuation, resulting in a relatively small range of the energy difference. Table 1 shows the irradiance thresholds defined by the threshold energy E_{t2} as well as the threshold input laser energies E_{t1} and E_{t2} for three different overpressures Δp. Figures 9 and 10 show the relationship between input laser energy, E_{in}, and the maximum bubble radius, R_{max}, for two overpressures (a) Δp=4.9kPa and (b) Δp=58.8kPa. It is obvious that a smaller bubble was generated when Δp is higher. Numerical calculations of the bubble energy E_B and shock wave energy E_S have been performed. We obtained the energy E_B to be 9-15% of Ec for Δp=4.9kPa and R_{max} =2.0mm, but a more careful consideration should be made when evaluating E_S.

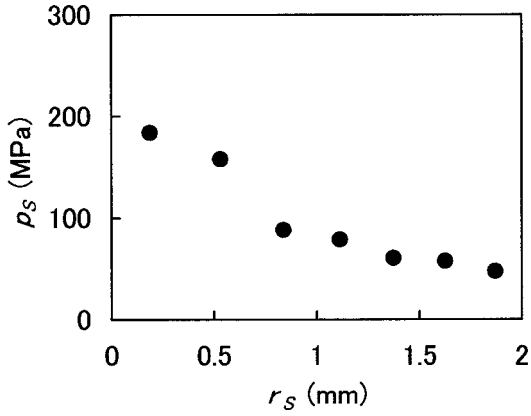

Figure 6. Shock wave pressure p_S calculated for Figure 5(b) with Δp=4.9kPa and R_{max}=2.08mm.

Table 1. Irradiance threshold I_{th} and the threshold input energies E_{t1} and E_{t2}

Δp [kPa]	E_{t1} [mJ]	E_{t2} [mJ]	E_{t2}—E_{t1} [mJ]	I_{th} [W/cm^2]
4.9	30.4	50.7	20.3	5.38 x 10^{11}
19.6	31.6	47.3	15.7	5.02 x 10^{11}
58.8	36.2	43.6	7.4	4.63 x 10^{11}

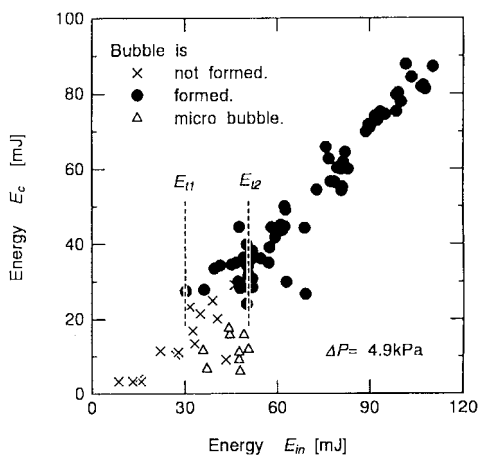

Figure 7. Input laser energy E_{in} versus the energy E_c consumed at the focus with Δp=4.9kPa.

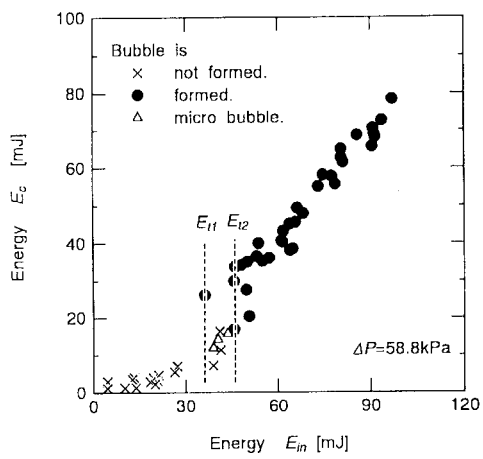

Figure 8. Input laser energy E_{in} versus the energy E_c consumed at the focus with Δp=58.8kPa.

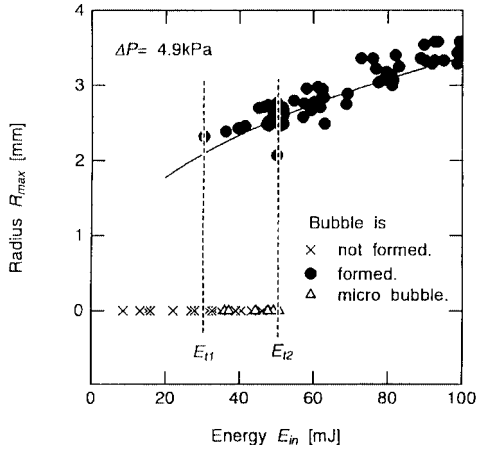

Figure 9. Input laser energy E_{in} versus maximum bubble radius R_{max} for Δp =4.9kPa.

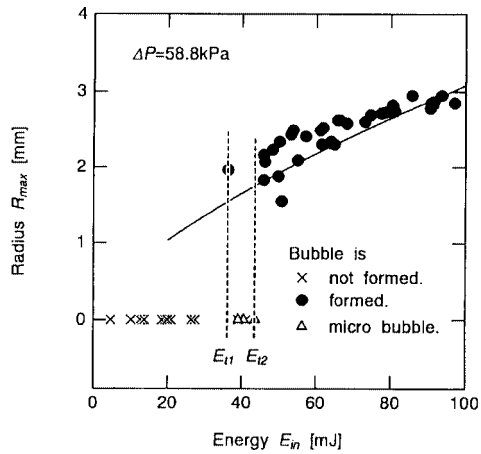

Figure 10. Input laser energy E_{in} versus maximum bubble radius R_{max} for Δp =58.8kPa.

5 Conclusions

The results obtained here are summarized as follows:

(1) There are two threshold energies, E_{t1} and E_{t2}, for bubble generation. For the input laser energy of $E_{in} \leq E_{t1}$ no bubbles were generated, while bubbles were always formed in the case of the input energy range of $E_{in} \geq E_{t2}$. When the input laser energy is between these two categories of energies, i.e. $E_{t1} \leq E_{in} \leq E_{t2}$, bubbles were generated with some probability depending on the homogeneities of liquid.

(2) The energy difference, E_{t1}–E_{t}, decreases as increasing Δp.

(3) The energies of bubble generation and shock wave emission have been investigated and evaluated in comparison with the input laser energy.

References

Angus, S., de Reuck, K.M. & Armstrong,B. 1977 *International thermodynamic tables of the fluids state – Volume 6 Nitrogen,* International Union of Pure and Applied Chemistry, Pergamon Press.

Barber, B.P. & Putterman, S.J. 1991 Observations of synchronous picosecond sonoluminescence. *Nature* **352**, 318.

Cole, R.H. 1948 *Underwater explosion.* . Princeton University Press.

Fujikawa, S. & Akamatsu, T. 1980 Effects of the non-equilibrium condensation of vapour on the pressure wave produced by the collapse of a bubble in a liquid. *J. Fluid Mech.* **97**, 481-512.

Gaitan, D.F., Crum,L.A., Church, C.C. & Roy, R.A. 1992 Sonoluminescence and bubble dynamics for a single, stable, cavitation bubble. *J. Acoust. Soc. Am.* **91**, 3166-3183.

Golubnitchii, P.I., Dyaduishkin, P.I., Kalugnii, G.C., Korchikov, S.D. & Kudlenko, V.G. 1979 Laser cavitation in liquid nitrogen. *PMTF* **5**, 103-106.

Isselin,J.-C., Alloncle, A.P. & Autric, M. 1998 On laser induced single bubble near a solid boundary: Contribution to the understanding of erosion phenomena. *J. Appl. Phys.* **84-10**, 5766-5771.

Lauterborn, W. 1974 Kavitation durch laserlicht. *Acustica* **31**, 51-78.

Maeno, K., Yokoyama, S., & Hanaoka, Y. 1990 Study on laser-induced cavitation bubbles in cryogenic liquids. *AIP Conf. Proc.* **208**, 383-388.

Mainster, M. A., Sliney, D.H., Belcher, C.D. & Buzney, S.M. 1983 Laser photodisruptors: Damage mechanisms, instrument design and safety. *Ophthalmology* **90**, 973-991.

Philipp, A. & Lauterborn, W. 1998 Cavitation erosion by single laser-produced bubbles. *J. Fluid Mech.* **361**,75-116.

Rayleigh Lord 1917 On the pressure developed in a liquid during the collapse of a spherical cavity. *Philos. Mag.* **34**,

94-98.

Sato, H., Sun, X.W., Odagawa, M., Maeno, K., Honma, H. 1996 An investigation on the behavior of laser induced bubble in cryogenic liquid nitrogen. *J. Fluids Eng*. **118**, 850-856.

Siegman, A.E., Sasnett, M.W. & Johnston, Jr. T.F. 1991 Choice of clip levels for beam width measurements using knife-edge techniques. *IEEE Journal of Quantum Electronics* **27-4**, 1098-1104.

Tomita, Y. & Shima, A. 1977 On the behavior of a spherical bubble and the impulse pressure in a viscous compressible liquid. *Bull. JSME* **20**, 1453-1460.

Tomita, Y. & Shima, A. 1990 High-speed photographic observations of laser-induced cavitation bubbles in water. *Acustica* **71**,161-171.

Tomita, Y., Shima, A., Tsubota, M. & Kano, I. 1994 An experimental investigation on bubble motion in liquid nitrogen. *Proceedings of 2nd International Symposium on Cavitation, Tokyo,* pp.311-316.

Tomita, Y., Tsubota, M., Nagane, K. & An-naka, N. 2000 Behavior of laser-induced cavitation bubbles in liquid nitrogen. *J.Appl. Phys*.**88-10**, 5993-6001.

Tsien, H.S. 1956 The Poincare-Lighthill-Kuo Method, *Advances in Appl. Mech*. **4**, 281-349.

Tsubota, M., An-naka, N. & Tomita, Y. 1996 High-speed fluid phenomena caused by laser beam focusing in liquid nitrogen. *SPIE* **2869**, 321-326.

Tsubota, M., Tomita, Y., Shima, A. & Kano, I. 1996 Dynamics of laser-induced bubble in pressurized liquid nitrogen. *JSME International Journal, Series B* **39-2**, 257-263.

Vogel, A., Busch, S. & Parlitz, U. 1996 Shock wave emission and cavitation bubble generation by picosecond and nanosecond optical breakdown in water. *J.Acoust. Soc. Am.* **100-1**, 148-165.

Vogel,A., Lauterborn,W. & Timm,R. 1989 Optical and acoustic investigations of the dynamics of laser-produced cavitation bubbles near a solid boundary. *J. Fluid Mech*. **206**, 299-338.

Vogel, A., Noack, J., Nahen, K., Theisen, D., Busch, S., Parlitz, U., Hammer, D.X., Noojin, G.D., Rockwell, B.A. & Birngruber, R. 1999 Energy balance of optical breakdown in water at nanosecond to femtosecond time scales. *Applied Physics B* **68**, 271-280.